ISSN 2179-3956

TRIBOLOGY OF FLUORINATED DIAMOND-LIKE CARBON COATINGS: FIRST PRINCIPLES CALCULATIONS AND SLIDING EXPERIMENTS[1]

F.G. Sen[2]
Y. Qi[3]
A.T. Alpas[2]

Abstract
Sliding contact experiments and first principles calculations were conducted to study tribological properties between aluminum and fluorinated diamond-like carbon (F-DLC) surfaces. Sliding tests between Al and F-DLC coating generated a low coefficient of friction (COF) of 0.1-0.14 and carbonaceous transfer layers containing AlF_3 were formed on the Al surfaces as determined by x-ray photoelectron spectroscopy. An interface model that examined interactions between Al (111) and F-terminated diamond (111) surfaces revealed that F atoms would transfer to the Al surface in increasing quantities with an increase in the contact pressure and the F transfer would lead to the formation of a stable AlF_3 compound at the Al surface. The generation of repulsive forces between two F-passivated surfaces as a result of F transfer to the Al surface resulted in attainment of a low COF between Al and F-DLC.
Keywords: Aluminum; Diamond-like carbon; Fluorine; First principles simulations.

[1] *Technical contribution to the First International Brazilian Conference on Tribology – TriboBr-2010, November, 24th-26th, 2010, Rio de Janeiro, RJ, Brazil.*
[2] *Department of Mechanical, Automotive and Materials Engineering, University of Windsor, Windsor, ON N9B 3P4 Canada*
[3] *Materials and Processes Laboratory, General Motors R&D Center, Warren, MI, 48090-9055 U.S.A.*

ISSN 2179-3956

1 INTRODUCTION

Diamond-like carbon (DLC) coatings are used to improve wear resistance in various applications, including biomedical applications, micro- and nano-electromechanical systems (MEMS/NEMS) and machining.[1,2] *(1, 2)*. DLC coatings' tribological properties depend primarily on the sp^3/sp^2 hybridization ratio of carbon bonds and their hydrogen content.[3] *(3)*. The incorporation of fluorine (up to 35 at%) decrease coefficient of friction (COF) and the surface energy of the DLC coatings.[4-6] *(4-6)*. Tribological properties of fluorinated DLC coatings (F-DLC) were reported to have optimum values for moderately [0.1< (F/F+C) <0.2] fluorinated films[6] *(6)* as shown by the sliding experiments.[4,5] *(4, 5)*.

The tribological properties of DLC coatings are also affected from the environmental conditions,[7] *(7)*, which have been generally discussed in terms of the dangling bonds of surface carbon atoms.[8] *(8)*. The passivation of dangling bonds by hydrogen or hydroxide group hinders interactions between surface carbon atoms and the environment, resulting in a stable surface and a low COF (<0.01).[8,9] *(8, 9)*. According to first principles calculations carried out at interfaces between aluminum and diamond, the passivation of diamond surfaces by -H *(10)* and –OH[8] *(8)* radicals created repulsive interactions between these surfaces and aluminum atoms. On the other hand, it was shown that aluminum atoms formed covalent bonds with surfaces consisting of carbon atoms that had exposed dangling bonds.[10] *(10)*. The formation of carbon rich transfer layers on the counterfaces that slid against H-DLC was identified as an important factor for attainment of low friction in DLC films.[11] *(11)*. It was suggested that after some material transfer from DLC to counterface, frictional interactions occur between two H-passivated surfaces, which according to the first principles calculations are very repulsive.[8] *(8)*. The first principles calculations also revealed that two F-passivated diamond surfaces facing each other would exert higher repulsive forces than two H-passivated surfaces and thus mutual interaction of two F-DLC surfaces would result in a lower COF.[12] *(12)*.

This study investigates friction and material transfer mechanisms between F-DLC and aluminum surfaces by conducting sliding experiments and characterizigin the contact surfaces. The interface strength between F-terminated diamond and aluminum surfaces was estimated from the first principles calculations. The effect that contact pressure had on material transfer was determined. The predictions of atomistic simulations at the interfaces were analysed together with the results of the sliding contact experiments to shed light on the effect of fluorine in carbon coatings in contact with aluminum surfaces.

2 SLIDING EXPERIMENTS

2.1 Experimental Procedure

The F-DLC and H-DLC coatings were deposited using a plasma assisted chemical vapour deposition (PACVD) system on M2 grade tool steel coupons in the form of 25.4 mm diameter discs. The carbon and fluorine compositions were determined using Rutherford backscattering spectroscopy (RBS), while the hydrogen composition was determined using the elastic recoil detection (ERD) technique. The properties of the F-DLC coatings and their elemental compositions are listed in Table 1.

ISSN 2179-3956

Table 1 Chemical composition and properties of F-DLC and H-DLC coatings. The thickness, *t*, was determined by Calotest. Surface roughness, R_a, was measured using a white light optical interferometer. Elastic modulus (*E*) and hardness (*H*) were measured using nanoindentation

	Chemical composition			Properties			
Coating designation	C (at %)	H (at %)	F (at %)	*t* (μm)	R_a (nm)	*E* (GPa)	*H* (GPa)
F-DLC	72	25	3	1.23±0.05	20±3	175±12	31±4
H-DLC	71	29	-	1.21±0.05	16±3	153±8	27±3

The F-DLC and H-DLC coated steel samples were placed in dry sliding contact against commercial purity (>99%) aluminum counterfaces in the shape of 6.35 mm diameter spherical balls, using a ball-on-disc type geometry as depicted in Figure 1. The aluminum balls were pressed on DLC surfaces at 1.0 and 10.0 N load under an ambient atmosphere with a relative humidity of 41±3% using a sliding speed of 0.12 m/s. A scanning electron microscope (SEM) equipped with an energy dispersive spectroscope (EDS) was used to examine the transfer layers generated on the Al surface. The composition of these layers was studied using X-ray photoelectron spectroscopy (XPS).

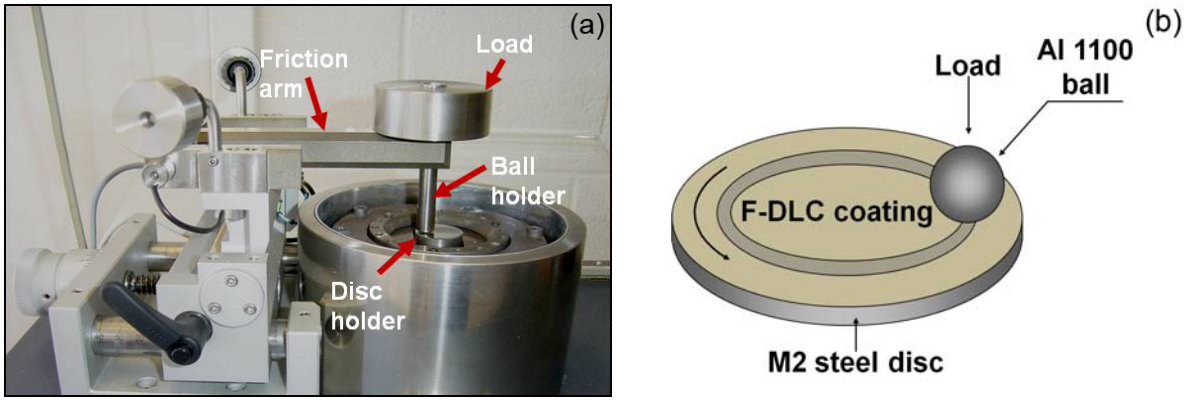

Figure 1. (a) The tribometer used in the sliding experiments and (b) the ball-on-disc geometry used.

2.2 Results of Sliding Experiments

The variation of the F-DLC coating's COF tested against Al with the sliding cycles under 1 N and 10 N load is shown in Figure 2. When 1 N load was applied, the COF of the F-DLC decreased continuously from an initially high COF of 0.60 to a steady-state value of 0.09±0.01 after 63 sliding cycles. For comparison the variation of the COF of H-DLC at 1 N applied load against Al is also plotted in Figure 2 which shows that H-DLC exhibited a higher COF of 0.14±0.01. Thus small amount of F decreased the COF by 36%. At 10 N load, at the beginning of the test, the COF was 0.54±0.06. The COF then reduced to a very low minimum value of 0.04±0.01 and gradually increased and stabilized at a value of 0.14±0.01 after 500 sliding cycles. The steady-state COF was maintained for the rest of a sliding test that lasted for 10^4 sliding cycles.

ISSN 2179-3956

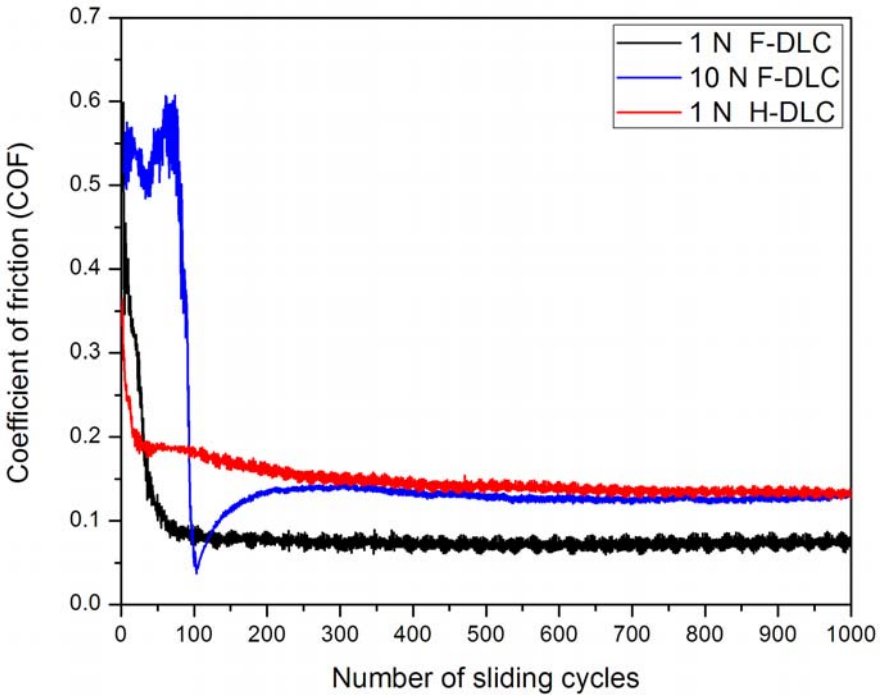

Figure 2. The variation in the COF of F-DLC sliding against Al under 1 N and 10 N applied loads. The COF of H-DLC sliding against Al under 1N is also shown.

Figure 3 (a) shows the SEM and EDS examination of the Al ball surfaces after the sliding test at 1 N load against F-DLC indicated that the Al surface was covered with a carbonaceous transfer layer. The high magnification image of this layer is given in Figure 3 (b). The SEM image of the Al surface after sliding against F-DLC at 10 N is shown in Figure 3 (c). It was observed that similar to the test at 1 N load, the Al surface was covered with a carbonaceous material. However, at 10 N load the Al surface was only partially covered by this material. The high magnification image of this layer (Figure 3 (d)) showed that the layer was thicker and denser than the layer formed at 1 N. Thus, the increase in the applied load promoted material transfer from F-DLC to Al. The EDS analysis of these transfer layers showed the presence of F in addition to C and O.

The XPS analyses of the transfer layer formed on Al surface showing the composition of the transfer layer is given in Figure 4 (a). The percentage of F in the transfer layer was 4.9 at% so that the F/C ratio in these transfer layers 0.09, which was higher than the F/C=0.04 in the as-deposited F-DLC coating. Therefore, F accumulated on the Al surface during sliding. High resolution XPS spectra of the transfer layers that recorded the binding energies of Al 2p are shown in Figure 4 (b). Accordingly, for the Al 2p spectra, a binding energy of 74.92 eV was assigned to the chemical state of Al_2O_3. Another important piece of information that the Al 2p spectra yielded, was the presence of AlF_3 that corresponded to a binding energy of 76.55 eV which matched with that of the AlF_3 reported in the literature,[13] *(13)*, inferring that the fluorine present in the DLC coating promoted the formation of AlF_3.

ISSN 2179-3956

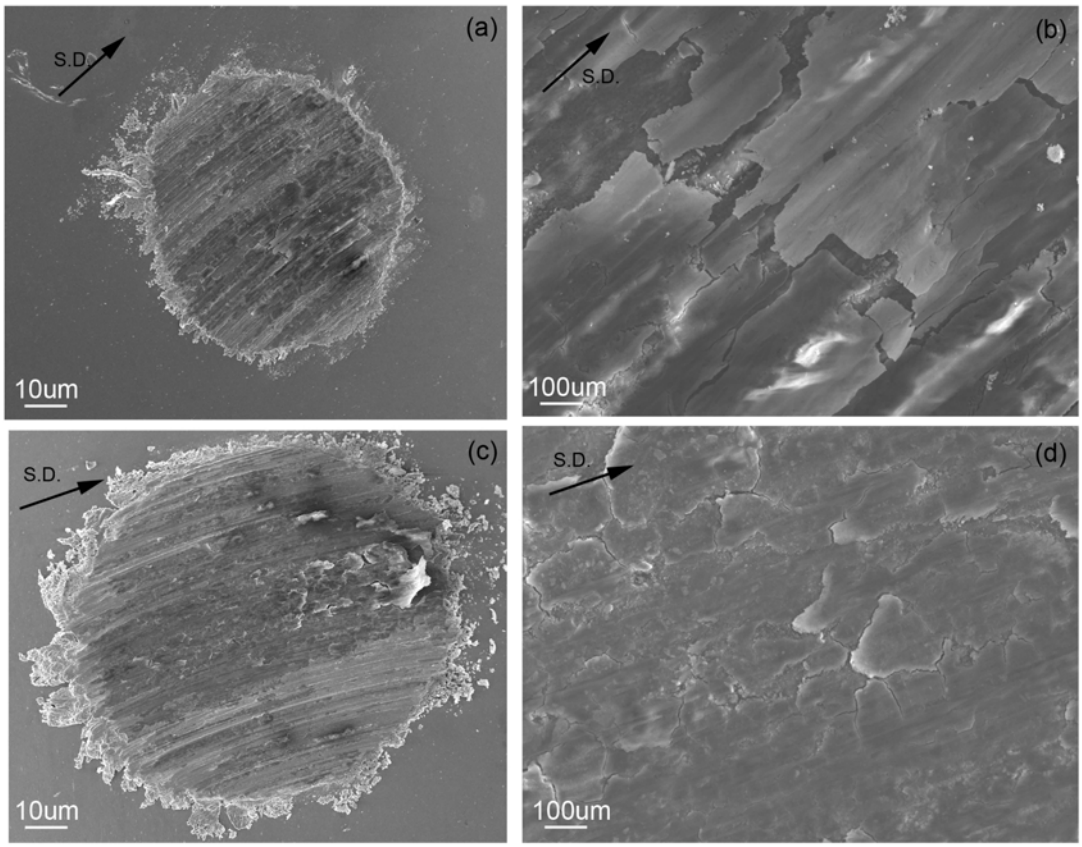

Figure 3. (a) Secondary electron image (SEI) of the Al ball surface after the sliding test against an F-DLC coating under 1 N load with an arrow indicating the sliding direction (S.D.) and (b) higher magnification image showing the transfer layer. (c) The SEI of the Al ball surface sliding under 10 N load and (d) higher magnification image of the transfer layers.

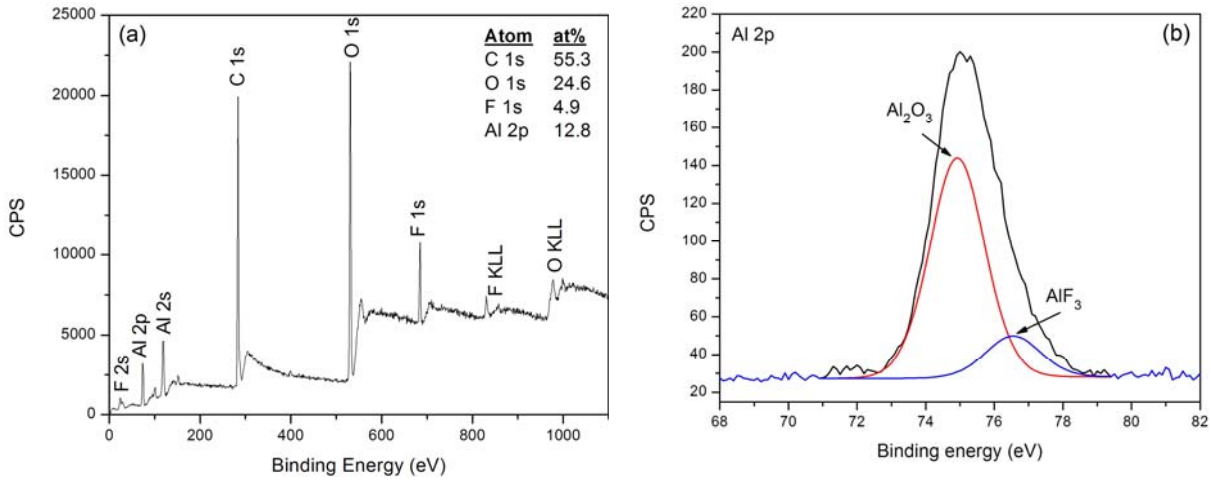

Figure 4. (a) The XPS survey scan of the transfer layers formed on Al surface after sliding against F-DLC. (b) The high resolution Al 2p XPS spectra of transfer layer with the deconvolution of the spectra to the chemical states of Al.

3 FIRST PRINCIPLES CALCULATIONS

3.1 Methodology

Interactions between Al and F-DLC surfaces were modeled using first principles calculations based on the density functional theory (DFT). All computations were performed using a projector augmented-wave (PAW) method and a generalized

ISSN 2179-3956

gradient approximation (GGA)[14] of exchange correlation energy, as implemented in the Vienna Ab initio Simulation Package (VASP).[15,16] The details of the computations can be found in elsewhere.[12]

The F-DLC coating surface was represented by an F-terminated diamond surface (diamond:F) by following the common practice in the literature of employing diamond to use as a model to study the DLC surfaces.[8,10] The convergence studies carried out revealed that use of six bi-layers of diamond:F and ten layers of Al (111) is sufficient for simulating the bulk effect in the each surface slab. The interface registry shown in Figure 5 (a) was constructed by matching a diamond:F (111)-(2x2) surface oriented in $[01\bar{1}]$ direction with an Al(111) surface oriented in $[\bar{1}2\bar{1}]$ direction to minimize the lattice mismatch. This configuration formed a hexagonal interface cell structure described by an orientation relationship of $(111)[\bar{1}2\bar{1}]_{Al} \parallel (111)[01\bar{1}]_{C}$ and consisted of a total of 86 atoms (Figure 5 (b)). The interface model consisted of a periodic arrangement of alternating diamond:F and Al layers without vacuum that had, and an inversion symmetry to ensure that both interfaces were the same.

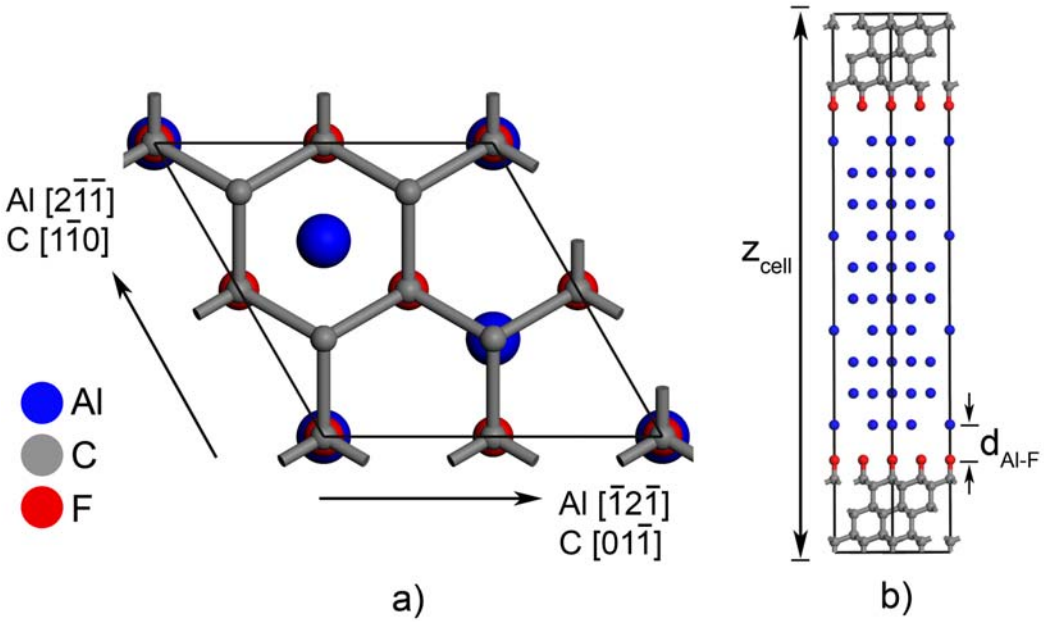

Figure 5. Al/diamond:F interface model. a) the top view of the interface registry (edge length of the cell is 5.05 Å). b) the side view showing 10 layers of Al and 6 bi-layers of diamond surface terminated with fluorine, where z_{cell} is the cell length and d_{Al-F} is the distance between the Al and F atoms.

Initially, atoms on Al and diamond:F surfaces were 8.8 Å apart. The interfacial separation distance (d_{Al-F}) was gradually decreased to 1.2 Å. The decrease in d_{Al-F} was accompanied by a decrease in the *z*-direction of the interface cell structure. For each intermediate separation distance considered and defined with respect to cell dimension z_{cell}, the total energy of the system (E_{tot}) was computed by letting the atoms relax in their initial positions without allowing the constrained interface cell structure to change. The change in E_{tot} was relative to that of the reference state E^{0}_{tot} at the far separated interface of $d_{Al-F} = 8.8$ Å i.e. $\Delta E_{tot} = \left(E_{tot} - E^{0}_{tot}\right)$. The surfaces were brought closer by applying an external pressure to the interfaces, so

ISSN 2179-3956

that the stress in the *z*-direction, σ_{zz}, normal to interface plane was: $\sigma_{zz} = -\frac{1}{A}\frac{\partial E_{tot}}{\partial z_{cell}}$ where *A*, the area of interface plane shown in Figure 5 (a), was equal to 22.1 Å^2. This stress can be regarded as the contact pressure exerted on the Al/ diamond:F interfaces.

3.2 Interface Energy Calculations

The change in ΔE_{tot} as a function of decreasing the separation distance between the Al and diamond:F surfaces, expressed as a function of z_{cell} is plotted in Figure 6 (a). The corresponding interfacial stress values at each z_{cell} was also plotted in Figure 6 (b). In Figure 6 (a) ΔE_{tot} initially reached a local minimum of -0.01 J/m^2 at $z_{cell} = 43.3$ Å, corresponding to $d_{Al-F} = 4.4$ Å, below which ΔE_{tot} started to rise—indicating occurrence of repulsion between Al and diamond:F. At $z_{cell} = 38.9$ Å ($d_{Al-F} = 2.8$ Å) ΔE_{tot} increased to a maximum of 0.45 J/m^2 and then dropped to 0.12 J/m^2 at $z_{cell} = 38.7$ Å. This reduction in ΔE_{tot} was accompanied by the transfer of an F atom to the Al surface. In this interface structure contact pressure was calculated to as $\sigma_{zz} = 3.5$ GPa (Figure 6 (b)). The 1 F transferred interface remained stable, until the ΔE_{tot} increased to 0.35 J/m^2 with the reduction in z_{cell} to 38.1 Å. For the interfaces that were pushed closer than this separation distance, the energy dropped to a global minimum of $\Delta E^{\min}_{tot} = -0.71$ J/m^2. At this point, the transfer of 3F atoms on the diamond surface to Al was occurred when $\sigma_{zz} > 4.5$ GPa (Figure 6 (b)). Finally, all 4 F atoms on the diamond surface became transferred to the Al side at $z_{cell} = 37.5$ Å when $\sigma_{zz} > 5.7$ GPa.

To determine the stability of the interfaces with 1F, 3F and 4F atoms transferred on the Al surface, the interface structures were pulled apart from their lowest energy configuration as designated by the dashed lines in Figure 6 (a) until the interfacial separations, d_{F-F} > 8.0 Å. ΔE_{tot} of the interfaces with the transferred F atoms had a lower energy compared to the original Al/diamond:F interface. This shows that the F transferred interfaces were more stable than the original interface structure. The separated interface energies provide evidence that the F transfer to the Al surface is a thermodynamically feasible process, and following the transfer of F atoms to Al prompted a repulsive interaction to be maintained between this surface and the diamond surface. It was concluded that F effectively passivated both surfaces. All F transferred interfaces had lower energy than the initial Al/diamond:F interface configuration with the 3F transferred interface being the most stable structure. In order to better understand the higher stability of 3 F transferred Al/diamond:F interface, the bonding structure of this interface was studied in detail and the results are reported in Section 3.3.

ISSN 2179-3956

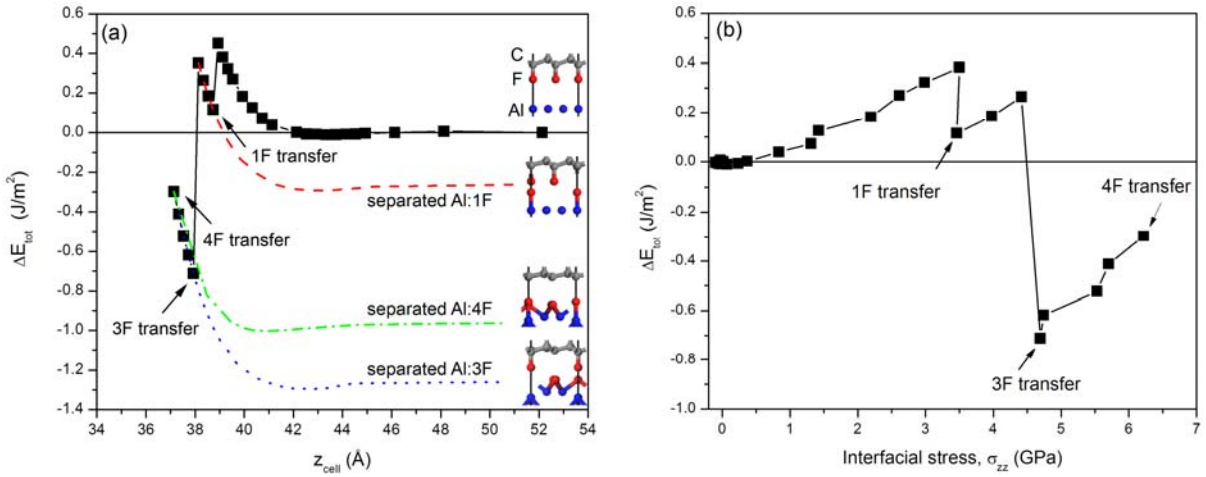

Figure 6. (a) The change in ΔE_{tot}, when an Al surface approaches diamond:F. ΔE_{tot} during separation of the F transferred Al/diamond:F interfaces were also plotted in dashed lines. The relaxed atomic structures of Al/diamond:F interfaces corresponding to initial interface, 1 F, 3 F and 4 F atom transfers to the Al surface were illustrated at z_{cell} at the insets. (b) The change in ΔE_{tot}, with respect to interfacial stress indicating the F transfers.

3.3 Bonding Structure of Interfaces and AlF_3 Formation

The bonding structure generated at Al/diamond:F interfaces was analyzed by using electron charge density difference analysis. The charge density differences between the interface and the diamond:F, and Al surface atoms in their corresponding structures were calculated. Figure 7 shows the electron charge density difference plot of the 3 F transferred Al surface in xy plane. The cut was made at the location of F atoms in the z-direction. Charge accumulations to F atoms and charge depletion from the Al atoms seen in Figure 7 indicate ionic bond formation between Al and F. When 3 F transferred to Al surface, two of the Al atoms became shifted away from their initial positions on the surface to bond with the three available F atoms--leaving only one non-bonded Al atom at the surface. As such, each Al atom was bonded to 3 F atoms as can be seen in Figure 7, which infers the possibility of an AlF_3 compound formation. The bond structure of the 3 F transferred Al surface was compared with the bond structure of the AlF_3 compound by relaxing the α-AlF_3 crystal *(17)*. In this structure, the Al-F bond distance was 1.82 Å and angles F-Al-F and Al-F-Al were 89.97º and 156.8º, respectively. When comparing the atomic arrangements of the AlF_3 crystal with the 3 F transferred Al surface, the Al-F bond distance (1.83 Å) and F-Al-F angle (88.4º) values (Figure 7) proved to be in excellent agreement. The Al-F-Al angle was higher in the AlF_3 crystal, because in the 3F transferred Al surface, only half of the AlF_6 octahedra was present.

ISSN 2179-3956

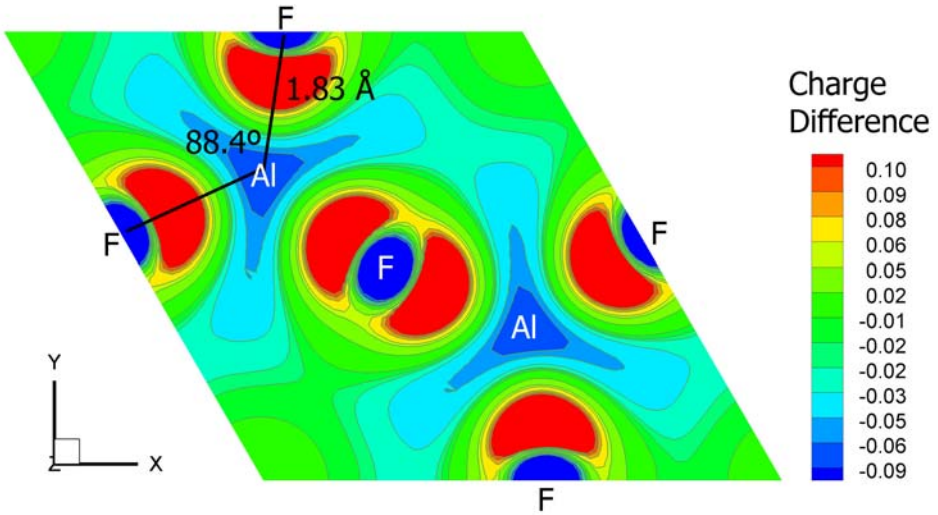

Figure 7. Charge density difference plot of reconstructed Al (111) surface after the transfer of three F atoms in xy plane while the plane cut was made at the locations of F atoms in the z-direction. Al and F atoms were not in-plane but Al atoms present at the under the F atoms relatively in the z-direction. Positive regions represent charge accumulation and negative regions show charge depletion.

In summary, first principles calculations predicted that F transfer at the Al/diamond:F interfaces was possible due to the application of high contact pressure. The F transfer was found to increase the interface stability, which was attributed to the surface reconstruction that occurred on the Al surface in the presence of F atoms. Analysis of the reconstructed Al surface provided support to the fact that AlF_3 would form at the Al surface.

4 DISCUSSION

The characterization of the contact surfaces when Al and F-DLC put in sliding contact experimentally and the use of first principles calculations served to illustrate the details of tribological nature of interactions between Al and F-DLC. When F-DLC was placed in contact against the Al surface, F atoms were transferred to the Al surface in accordance with the predictions of the first principles calculations. These calculations suggested that when an Al and a diamond:F surface were brought together, the sequence of atomic transfer events would occur in the manner described in Figure 6, and eventually all F atoms at the diamond surface would transfer to the Al surface.

The high COF during the initial contact can be attributed to the chemical attraction between the Al and F at the surface under high contact pressure. F transfer to Al is accompanied by breaking of the C-F bonds and formation of new Al-F bonds at the contact surfaces, both processes consume energy and may contribute to the initial high COF period *(18)*. During the material transfer to Al, C bonds in the F-DLC structure are broken, and a C transfer to Al occurs. The transfer of F atoms to Al cause the formation of stable Al/diamond:F interfaces that develop repulsive forces between themselves when pulled apart (Figure 6). AlF_3 surfaces are expected to assume an F termination *(19)*. Hence, the formation of AlF_3 would contribute to the F passivation of the transfer layer that formed on the Al surface. Consequently, once F-containing transfer layers are established, only a small friction force between the surfaces in contact is expected to arise. Experimentally, this is proven to be the case by the low COF observed in the steady state regime of the friction curves in Figure 2.

ISSN 2179-3956

According to the first principles calculations, the number of F atoms transferred to the Al would increase with an increase in the contact pressure (Figure 6 (b)). During the sliding tests, the increase in the material transfer at high load (10 N) yielded a very low COF (0.04), but due to high contact pressure the transfer layers could not remain intact at the contact interface which resulted in an increase in the COF. It was reported that a steel surface sliding against F-DLC produced an increase in the amount of transfer from fluorine containing carbon to steel when the contact pressure increased,[4] while metal fluoride formations were observed on metals sliding against PTFE.[20,21] Consequently, tribological mechanisms between Al and F-DLC in this study should be applicable to any metal and fluorinated carbon surfaces in contact.

5 CONCLUSIONS

Sliding experiments and first principles calculations were carried out in order to provide insight into the tribological behaviour of the Al and F-DLC coating system. The main conclusions of this work can be summarized as follows:

1. Sliding contact tests of F-DLC coatings against Al at high applied load indicated an initially high COF. But once carbonaceous material transfer to Al occurred, the COF dropped to a low COF value.
2. First principles calculations using an interface model consisting of diamond:F (111) surface and Al (111) interfaces predicted that F atoms would transfer to the Al when the contact pressure at the interface > 3.5 GPa. Higher contact pressures yielded more F transfer to Al.
3. The XPS analysis of the transfer layers formed on the Al surface revealed the formation of AlF_3 compound during sliding contact. The formation of this compound was predicted by the first principles calculations as a result of analyses of the bond structure of the F transferred Al surfaces.

Acknowledgments

This work is supported by NSERC (National Science and Engineering Research Council of Canada) and General Motors of Canada Ltd. Computations were carried out using the facilities at the SHARCNET (Shared Hierarchical Academic Research Computing Network). DLC coatings were obtained from Bekaert Advanced Coatings Ltd., New York.

REFERENCES

1 Grill, A. Diamond-like carbon: State of the art. **Diamond. Relat. Mater.**, n. 8, p. 428-434, 1999.
2 Erdemir, A.; Donnet, C. Tribology of diamond-like carbon films: recent progress and future prospects. **J. Phys. D Appl. Phys**., n. 39, p. R311-R327, 2006.
3 Robertson, J. Diamond-like amorphous carbon. **Mater. Sci. Eng. R**, n 37, p. 129-281, 2002.
4 Donnet, C.; Fontaine, J.; Grill, A.; Patel, V.; Jahnes, C.; Belin, M. Wear-resistant fluorinated diamondlike carbon films. **Surf. Coat. Tech.**, n. 94-95, p. 531-536, 1997.
5 Hakovirta, M.; He, X. M.; Nastasi, M. Optical properties of fluorinated diamond-like carbon films produced by pulsed glow discharge plasma immersion ion processing. **J. Appl. Phys.**, n. 88, p. 1456-1459, 2000.

ISSN 2179-3956

6 Donnet, C. Recent progress on the tribology of doped diamond-like and carbon alloy coatings: A review. **Surf. Coat. Tech**., n. 100-101, p. 180-186, 1998.
7 Andersson, J.; Erck, R. A.; Erdemir, A. Frictional behavior of diamondlike carbon films in vacuum and under varying water vapor pressure. **Surf. Coat. Tech**., n. 163-164, p. 535-540, 2003.
8 Qi, Y.; Konca, E.; Alpas, A. T. Atmospheric effects on the adhesion and friction between non-hydrogenated diamond-like carbon (DLC) coating and aluminum - A first principles investigation. **Surf. Sci.**, n. 600, p. 2955-2965, 2006.
9 Erdemir, A. The role of hydrogen in tribological properties of diamond-like carbon films. **Surf. Coat. Tech**., n. 146-147, p. 292-297, 2001.
10 Qi, Y.; Hector, L. G. Adhesion and adhesive transfer at aluminum/diamond interfaces: a first-principles study. **Phys. Rev. B**, n. 69, p. 235401, 2004.
11 Ronkainen, H.; Likonen, J.; Koskinen, J.; Varjus, S. Effect of tribofilm formation on the tribological performance of hydrogenated carbon coatings. **Surf Coat Technol.**, n. 79, p. 87-94, 1996.
12 Sen, F. G.; Qi, Y.; Alpas, A. T. Surface stability and electronic structure of hydrogen- and fluorine-terminated diamond surfaces: A first-principles investigation. **J. Mater. Res.**, n. 24, p. 2461-2470, 2009.
13 Moulder, J. F.; Stickle, W. F.; Sobol, P. E.; Bomben, K. D. **Handbook of X Ray Photoelectron Spectroscopy**; Physical Electronics: Chanhassen, MN, 1995.
14 Perdew, J. P.; Chevary, J. A.; Vosko, S. H.; Jackson, K. A.; Pederson, M. R.; Singh, D. J.; Fiolhais, C. Atoms, molecules, solids, and surfaces: Applications of the generalized gradient approximation for exchange and correlation. **Phys. Rev. B**, n. 46, p. 6671-6687, 1992.
15 Kresse, G.; Hafner, J. Ab initio molecular-dynamics simulation of the liquid-metalamorphous- semiconductor transition in germanium. **Phys. Rev. B**, n. 49, p. 14251-14269, 1994.
16 Kresse, G.; Furthmüller, J. Efficiency of ab-initio total energy calculations for metals and semiconductors using a plane-wave basis set. **Comput. Mater. Sci**., n. 6, p. 15-50, 1996.
17 Daniel, P.; Bulou, A.; Rousseau, M.; Nouet, J.; Fourquet, J. L.; Leblanc, M.; Burriel, R. A study of the structural phase transitions in AlF3: X-ray powder diffraction, differential scanning calorimetry (DSC) and Raman scattering investigations of the lattice dynamics and phonon spectrum. **J. Phys. Cond. Matter**, n. 2, p. 5663-5677, 1990.
18 Pastewka, L.; Moser, S.; Moseler, M.; Blug, B.; Meier, S.; Hollstein, T.; Gumbsch, P. The running-in of amorphous hydrocarbon tribocoatings: A comparison between experiment and molecular dynamics simulations. **Int. J. Mater. Res**., n. 99, p. 1136-1143, 2008.
19 Bailey, C. L.; Mukhopadhyay, S.; Wander, A.; Searle, B. G.; Harrison, N. M. Structure and stability of r-AlF3 surfaces. **J. Phys. Chem. C**, n. 113, p. 4976-4983, 2009.
20 Brainard, W. A.; Buckley, D. H. Adhesion and friction of PTFE in contact with metals as studied by Auger spectroscopy, field ion and scanning electron microscopy. **Wear**, n. 26, p. 75-93, 1973.
21 Cadman, P.; Gossedge, G. M. The chemical nature of metal-polytetrafluoroethylene tribological interactions as studied by X-ray photoelectron spectroscopy. **Wear**, n. 54, p. 211-215, 1979.